



OPEN

Cytotoxic potential of *Curcuma caesia* rhizome extract and derived gold nanoparticles in targeting breast cancer cell lines

Ajoy Kumar Das^{1,2✉}, Maina Borah³, Jon Jyoti Kalita² & Utpal Bora^{2✉}

Among all types of cancer, breast cancer is the most aggressive, as it is responsible for most of the cancer related death of women. Though several medical therapies are available, the scenario of curing such disease is not favorable. Therefore, there is an urgent need to find alternatives to deal with it. The knowledge of ethnopharmacy might give some better solution to mitigate such deadly diseases. Here, we are using the rhizome of *Curcuma caesia* Roxb. (Black turmeric), as well as gold nanoparticles (GNPs) synthesized with it to check their specific cytotoxic potentiality against breast cancer cell lines. In our study, ethanolic extract was used to evaluate the cytotoxic effect of the rhizome. GNPs were synthesized by using the same extract and characterized by UV–Vis spectroscopy (UV–Vis), Transmission electron microscopy (TEM), X-ray diffraction (XRD), Fourier-transform infrared spectroscopy (FTIR), and Thermo gravimetric analysis (TGA). The TEM, XRD, FTIR and TGA results revealed the successful synthesis and capping of GNPs. The UV–Vis Spectrum showed a sharp and narrow absorption peak at 550 nm and HRTEM confirmed both the stability and successful synthesis of the nanoparticles. The MTT assay of the crude extract revealed strong cytotoxicity against breast cancer cell lines viz. MCF-7 (ER⁺) and MDA MB-231 (Triple Negative Breast Cancer, TNBC) by showing IC₅₀ values as 15.70 ± 0.029 and 21.57 ± 0.031 µg/mL respectively. For extract mediated GNPs, the IC₅₀ values were found to be 6.44 ± 0.045 and 5.87 ± 0.031 µg/mL respectively in both breast cancer cell lines. As the IC₅₀ value for GNPs was found to be much lower than that of crude extract, it indicates a higher efficiency of the GNP. However, both the rhizome extract and its mediated GNPs showed more toxicity towards MDA MB-231 (TNBC) cell lines. It was also observed that the GNPs showed more toxicity towards TNBC cell lines compared to the rhizome extract. No toxicity was found in case of other cell lines such as L 929 and HeLa for both crude extract as well as for GNPs. These observations suggests that both the crude rhizome extract and its derived GNPs exhibit selective cytotoxic potential against breast cancer cell lines, which might be exploited for target specific treatment. Moreover, with an understanding of the mechanism behind the GNPs therapeutic efficiency, it can be developed as a personalized therapy to treat such type of cancers.

Keywords Breast cancer, Cytotoxicity, Black turmeric, GNPs

Curcuma caesia Roxb. (Black turmeric) is a perennial herb and is endemic to North East and central India¹. It is widely cultivated in South East Asian countries and the rhizome of this plant is extensively used in folk medicine in this region^{2,3}. The rhizome of black turmeric contain sar-turmerone, (Z)-ocimene, camphor, 1, 8-cineole, borneol, elemene, bornyl acetate, curcuzederone, curcumin, and curcumin as the main elements^{4,5}. It is used for curing myriad of ailments including cancer, haemorrhoids, epilepsy, leprosy, impotency, gonorrhoea and asthma etc. It is also used as central nervous system (CNS) depressant, locomotor depressant and smooth muscle relaxant^{6–9}. Curcuminoid and curcuzederone, which are the major component of the rhizome of this species, are used particularly in breast cancer treatment^{10–13}. The *in-vivo* antitumor activity of ethanolic extract of *Curcuma caesia* rhizome and curcuzederone (one of its compound) has already been reported against Ehrlich ascites

¹Department of Botany, Arya Vidyapeeth College (Autonomous), Gopinath Nagar, Guwahati, Assam 781 016, India. ²Department of Biosciences and Bioengineering, Indian Institute of Technology Guwahati, Guwahati, Assam 781 039, India. ³Department of Botany, Pandu College, Guwahati, Assam 781 012, India. ✉email: ajoykradasvc@gmail.com; ubora@iitg.ernet.in

carcinoma and triple negative breast cancer^{14–16}. Though this plant has enough potentiality in pharmaceutical and therapeutic value this plant is now categorised as critically endangered species due to over exploitation¹⁷. Therefore, this plant is quite important from the conservation and medicinal point of view. Again, exploration of its potentiality towards cytotoxic in breast cancer might help in developing new horizon in treatment of such aggressive disease.

In recent years, nanotechnology has gained attention in various fields including textiles, electronics, energy, defence, catalysis, agriculture, food, water treatment and medicine¹⁸. Now, the use of nanomaterials in health-care is considered as one of the most promising approach. As the nanoparticles are biocompatible, highly bio-available and more precise, it has been drawing huge attention in the field of biomedical sciences specifically in bioimaging, drug delivery and cancer therapy^{18,19}. Moreover, functionalization of such particles promote the interactions with different biomolecules thereby enhances its efficacy and reactivity^{20–22}. Among different techniques of synthesis, green method has gained a wider acceptance as it is cost-effective, eco-friendly, stable and easy to store²³. However, apart from its ample advantages, due to its smaller size and high surface-volume ratio, it exhibits high toxic effects to human health and to the environment²⁴. As the adsorption of biomolecules and ions is determined by the surface area of the particles, it elicits the cell responses and thereby induces toxicity⁸. Furthermore, the shapes and structures also contribute to nanotoxicity. Certain nanopartilces, such ceramic particles used in drug delivery, have been reported to induce oxidative stress in liver, lungs, brain and heart as well as carcinogenic activities²⁵. It also affects the environment due to rapid release of nanoparticles to it. Yet, the toxicity mechanism and the assessment of such particle are still not clear²⁶.

Nanomaterial like the gold nanoparticles (GNPs) have drawn more interest due to its unique properties such as high optoelectrical as well as surface plasmon scattering properties, flexibility in tuning sizes, ease of modification. The unique physico-chemical properties of GNPs make them a potential agent in drug delivery system, cell imaging as well as in curing cancer^{27–34}. The surface plasmon resonance (SPR) properties of GNPs make them an attractive contender in radiation therapy for cancer^{35,36}. Although it is an attractive candidate to resolve different therapeutic issues, it has been reported that such particles have certain potential impact on environment and health^{37,38}. Its size and shape as well as its surface coating play a crucial role in determining toxicity³⁹. Additionally, its small size and high surface area-volume ratio helps it to cross any physical barrier of the body system and thereby interact with different organs such as spleen, liver, brain^{40,41}. In this context, an elevated level of accumulation and oxidative damages has already been reported in liver, spleen and other organs. Due to exposure during synthesis, applications and disposal it also accumulates in the environment and thus affects the whole food chain⁴². Generally, in therapeutic application, non-toxic, inert and easily dispersible GNPs are preferred⁴³. Here, green chemistry method has been found to be advantageous over other available physical and chemical method of GNPs synthesis since it is eco-friendly and cost-effective^{44,45}. Natural source, plant materials are preferentially used as reducing and capping agent in green synthesis of GNPs. Phytochemicals of plants such as alkaloids, flavonoids, terpenoids and steroids are mainly responsible for the reduction of metal ion to its stable oxidative state⁴⁶. The functional groups, basically carboxylic (–COOH), amide (–NH₂C=O), hydroxyl (–OH) and carbonyl (C=O) etc. present in different phytochemicals have the ability to reduce and stabilize the ions through their hydrogen bonding, π – π bonding and electrostatic interactions capacity⁴⁷.

The overall mechanism of synthesis of metal nanoparticles using plant extract mainly consists of four steps. In the first activation phase, ionization of the metal takes place in aqueous medium and these ions are trapped by the functional groups of the phytochemicals through electrostatic interactions between metal ions and the functional groups. In the next step, nucleation (metal nuclei) takes place through reduction of the metal ions attracted by the functional groups with the help of electron transfer. This second step is followed by the growth phase, where adjoining nanoparticles coalesce to form large sized particles through heterogenous nucleation process (Ostwald ripening process). In this step, the large sized nanoparticles also become thermodynamically stable. The last growth termination step involves capping of accumulate nanoparticles by the functional groups present in the phytochemicals^{48–50}. However, as different phytochemicals are involved to reduce mono or divalent metal ion into zero valent state (nano form), the particular mechanism of reduction is yet to be explained.

Plant derived GNPs have shown various functions in biomedical field such as antiviral, antimicrobial, anti-oxidant, anticancer and anti-inflammatory activities⁵¹. Recently, the plant mediated GNPs have brought different significant advancement in diagnosis and treatment of cancer⁵². Different plant species have been exploited to synthesize GNPs and to verify their biomedical applications. Curcumin encapsulated with GNPs as well as other polymeric nanoparticles have been reported to exhibit enhanced bioavailability⁵³. However, the efficacy of the crude rhizome extract and its mediated synthesized GNPs of *Curcuma caesia* Roxb. (Black turmeric), which is endemic to North East India has been not studied so far. In our study, we investigated the specific *in-vitro* anti-cancer activity of ethanolic extract of its rhizome (EER) as well as EER mediated synthesized GNPs (synthesized at room temperature) on ER⁺ and TNBC cell lines (MCF-7 and MDA MB-231) as well as on different mammalian cell lines including HeLa and L929.

Breast cancer is the second leading cause of death in woman which accounts 22.9% of all cancer^{54,55}. In developing country, the survival rate of the breast cancer patients is very poor. In India, one in 22 women has the possibility to be suffered from breast cancer during her lifetime⁵⁶. The GNPs, synthesized using the rhizome extract of this plant might be a potential candidate in the treatment of breast cancer.

Results and discussion

Cytotoxic potential of EER

The anticancerous property of the EER was tested against four different cell lines including one normal cell line (L929) through tetrazolium assay (MTT). Different concentrations of the drugs ranging from 0.5 to 200 μ g/mL were used for the test. The EER showed no cytotoxic effects for cell lines L929 and HeLa (Fig. 1). A high viability

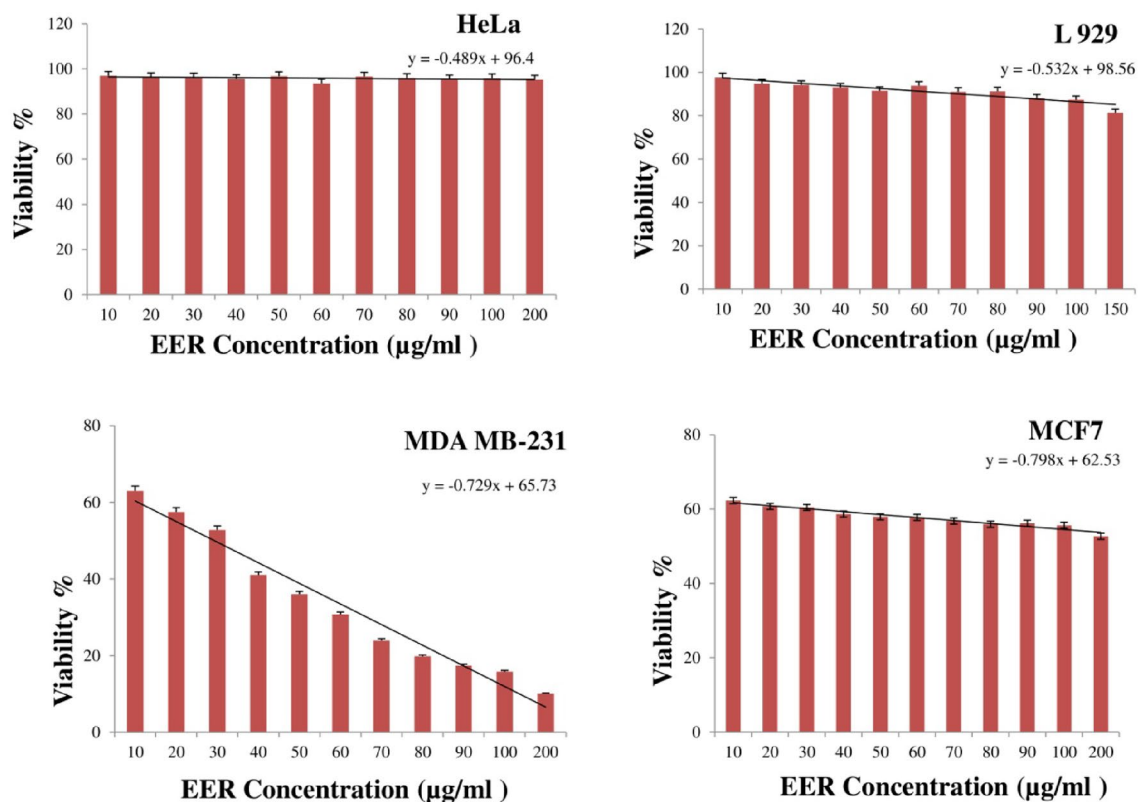


Figure 1. Cytotoxicity of EER on HeLa, L929, MDA MB -231 and MCF-7 cell lines.

of the cells was observed for both these cell lines ($93.83 \pm 4.2\%$ and $96.71 \pm 3.9\%$ respectively). IC_{50} values for both the cell lines were obtained as 91.27 ± 0.046 and 94.80 ± 0.038 $\mu\text{g/mL}$ respectively (Table 1). But, interestingly, the MTT assay revealed strong cytotoxicity against the breast cancer cell lines, MCF-7 (ER⁺) and MDA MB-231 (TNBC) respectively (Fig. 1). The IC_{50} values for both MCF-7 and MDA MB-231 were found as 15.70 ± 0.029 and 21.57 ± 0.031 $\mu\text{g/mL}$ respectively (Table 1). In our investigation, the cell viability was observed to be decreased with the increase of concentrations of EER (Fig. 2). Similar result was observed for zerumbone, one of the major constituents of *Curcuma caesia*. The IC_{50} value for zerumbone in case of MCF-7 and MDA MB-231 was found as 13.0 ± 0.8 , 25.2 ± 1.5 mM⁵⁷. Significant antimigratory effect against MCF-7 and MDA MB-231 was also shown by the bark extract of *Albizia lebbeck*⁵⁸. The ethanolic leaf extract of *Annona muricata* and *Lantana camara* showed similar result on MCF-7 as well as on MDA MB-231 respectively^{59,60}. Extract of *Sambucus ebulus* showed a satisfactory antiproliferative effect against triple negative breast cancer⁶¹. IC_{50} value less than 30 $\mu\text{g/mL}$ is considered as the highly cytotoxic according to the guidelines of National Cancer Institute (NCI)^{62,63}. However, in our study, the EER showed more toxicity towards MDA-MB 231 (TNBC) cell lines (Figs. 1 and 2). This is might be due to the presence of functional groups of the rhizome which are more specific in action towards the TNBC cell lines. Thus, the present study indicates the potential breast cancer specificity of EER. Strong cytotoxicity of EER of this plant against triple negative breast cancer (MDA MB-231) was in accordance with the findings of earlier reports^{12,64}. The understanding of the exact mechanism behind the specificity of the rhizome extract towards TBNC toxicity might help in formulating traditional medicine in near future.

Name of the Cell lines	Type of Treatment	IC50 Value ($\mu\text{g/mL}$)
L929	EER	91.27 ± 0.046
HeLa	EER	94.80 ± 0.038
MCF-7(ER ⁺)	EER	15.70 ± 0.029
MDA MB-231	EER	21.57 ± 0.031
L929	GNP	90.08 ± 0.021
HeLa	GNP	94.18 ± 0.034
MCF-7(ER ⁺)	GNP	6.44 ± 0.045
MDA MB-231	GNP	5.87 ± 0.031

Table 1. Comparison IC_{50} values of EER and GNPs on studied cell lines.

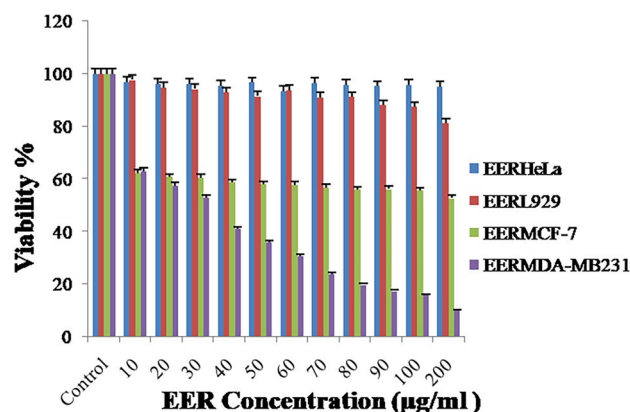


Figure 2. Effect of different concentration of EER and negative control on on HeLa, L929, MDA MB-231 and MCF-7 cell lines.

Synthesis of GNPs

The EER mediated synthesized GNPs were characterized by UV–vis spectroscopy, Transmission electron microscopy, X-ray diffraction, Fourier-transform infrared spectroscopy and Thermo gravimetric analysis.

UV–VIS absorbance spectroscopy

The synthesis of GNPs was ensured from the colour change of the reaction mixture from yellow to ruby red colour. Synthesis of GNPs was confirmed with a UV–vis spectrophotometer. A distinct surface plasmon resonance (SPR) band with sharp and narrow peak was observed centred at around 550 nm (Supplementary Information, S1). Optimum condition for synthesis of GNPs were observed as 1.2% (v/v) EER, 1.5 h reaction time and 0.875 mM gold solution as shown in the Supplementary Information, S1.

Transmission electron microscopy (TEM)

TEM analysis of the optimized reaction mixture revealed that nanoparticles were of spherical and hexagonal in shape (Fig. 3). The ultra high-resolution TEM (UHRTEM) image and selected area electron diffraction (SAED) pattern showed clear lattice fringes and bright rings corresponding to (1 1 1), (2 0 0), (2 2 0) and (3 1 1)

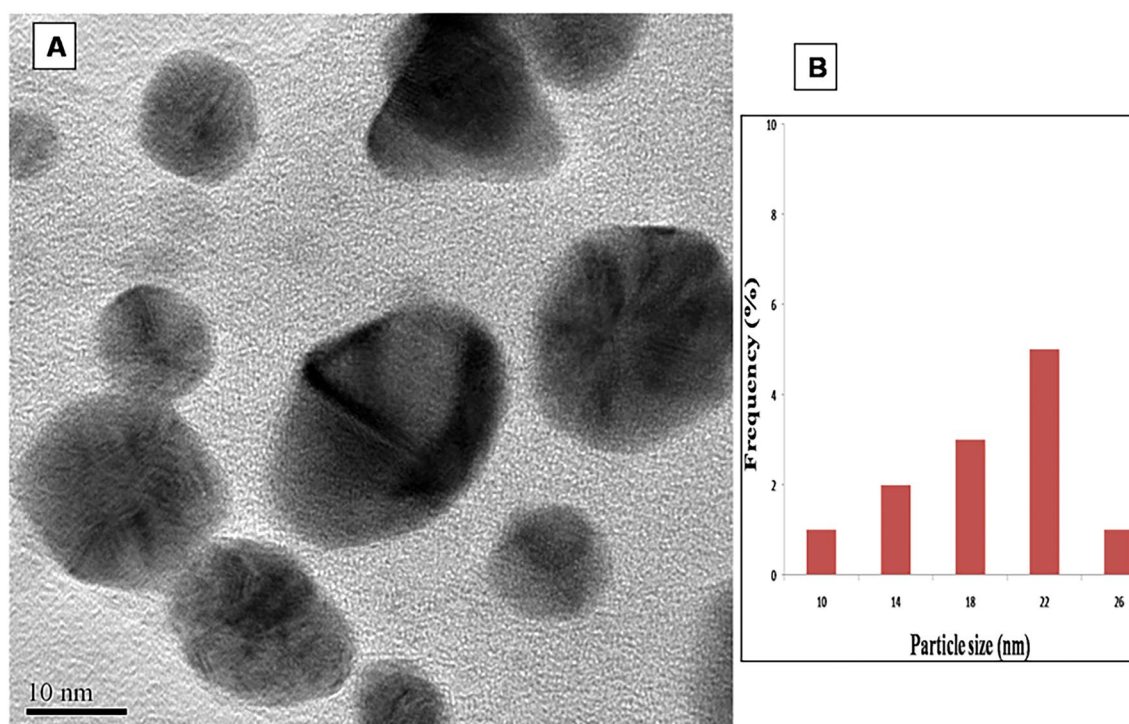


Figure 3. (A) TEM image of GNPs, (B) Histogram showing size distribution of GNPs.

respectively which confirmed the crystal nature of GNPs (Figs. 4, 5). The size of the particles varied from 10 to 26 nm (Fig. 3). The average particle size was found to be 18 ± 2.095 nm.

X-ray diffraction (XRD) analysis

XRD pattern of synthesized GNPs showed four prominent Bragg reflections at the intensities of (1 1 1), (2 0 0), (2 2 0) and (3 1 1) which were indexed on the basis of fcc structure of gold crystal planes (Fig. 5).

Fourier transform infrared spectroscopy (FTIR)

The FTIR spectrum of EER revealed characteristic IR bands for C=O stretching vibration for ester group (1049.3 cm^{-1} , 1095.6 cm^{-1}), for C–H stretching for alkanes (2981.0 cm^{-1}), hydrogen bonded O–H stretch for phenols/alcohols (3479.6 cm^{-1}) functional groups. Band at 1714.7 cm^{-1} indicates the vibration of carbonyl group (Curve 1, Fig. 6A). All these bands were likely originated from different phytochemicals present in the EER.

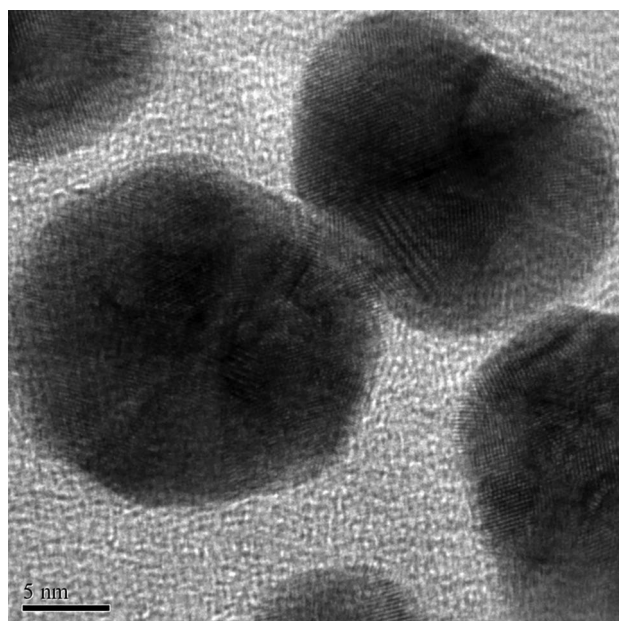


Figure 4. HRTEM image of GNPs.

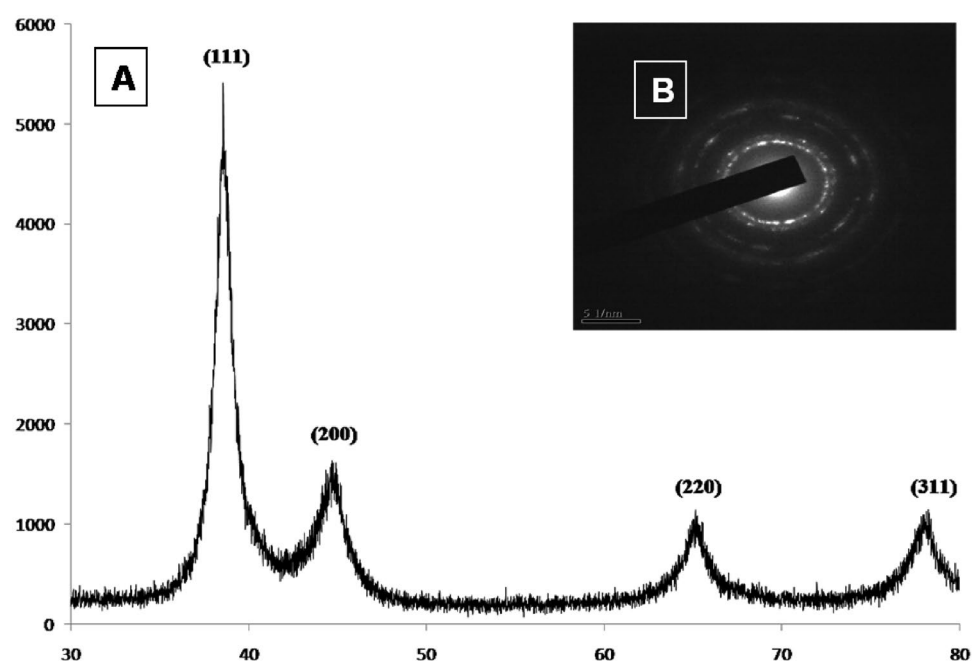


Figure 5. (A) XRD analysis of GNPs, (B) SAED pattern of GNPs.

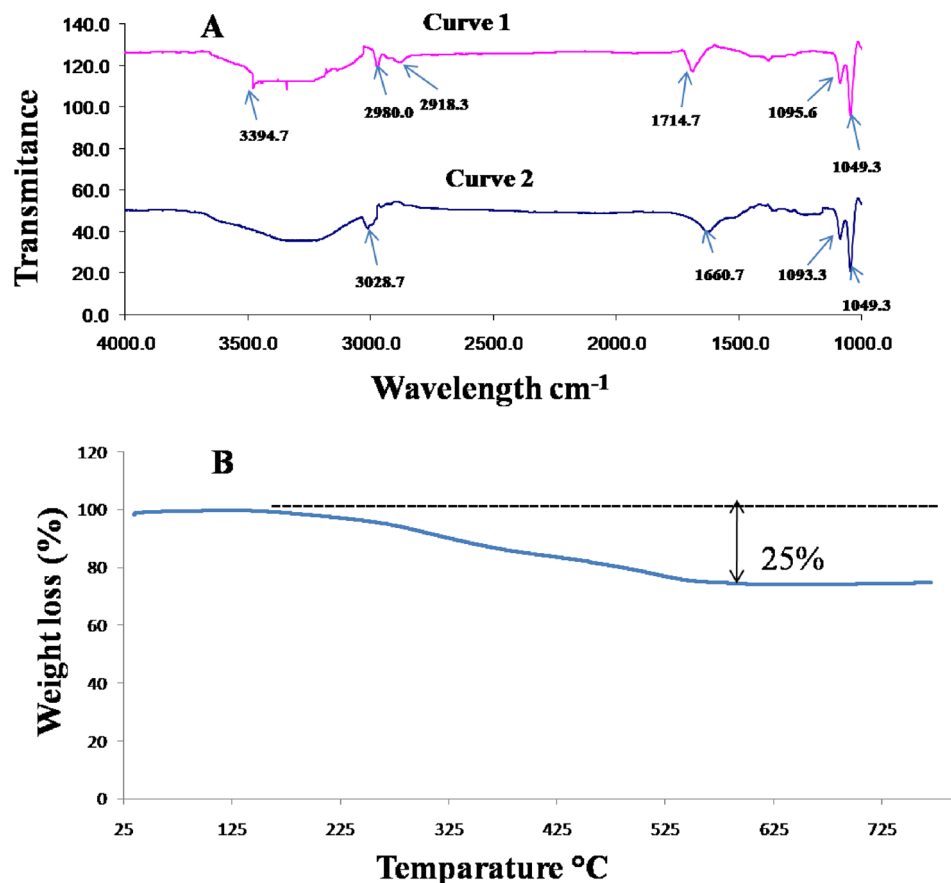


Figure 6. (A) FTIR of EER (Curve 1) and GNP (Curve 2) 5 (B) TGA analysis of GNPs.

Appearance of IR band at 1049, 1095 and 2981.0 cm⁻¹ unveiled the distinctive absorption of polysaccharides present in the endangered plant species. Polysaccharides are generally responsible for the enhancement of body immunity, antitumor activity and confronting damage due to radiation³⁴. FTIR spectrum of lyophilized GNPs showed almost common IR bands to EER (Curve 2, Fig. 6A). Distinct IR bands corresponding to ester, alkanes, as well as carbonyl functional groups were found to be observed for GNPs. The FTIR analysis gives the strong evidence of capping behaviour of EER which makes GNPs highly stable.

Thermo gravimetric analysis (TGA) analysis

The temperature of the TGA spectra ranged from 158 to 725 °C. TGA spectral analysis revealed substantial weight loss of GNPs which suggests the degradation of the bioactive molecules capped on GNPs due to high temperature (Fig. 6B).

Cytotoxicity of GNPs

MTT assay was performed to evaluate the cytotoxicity of the synthesized GNPs for the same four cancer cell lines using different concentrations (0.5 to 200 µg/mL). Similar result was found to be observed as that of EER. The MTT assay revealed strong cytotoxicity against both breast cancer cell lines, MCF-7 and MDA MB-231, but no toxic effect for L929 as well as HeLa (Fig. 7). Similar result was observed for iron oxide nanoparticles synthesized by methanolic extract of *Moringa oleifera*. The spherical *M. oleifera* mediated iron oxide NPs showed potential antiproliferative and cytotoxic effect against MDA MB-231⁶⁵. Similarly, aqueous leaf extracts of *Cordia myxa* L. and *Ziphus spina-christi* showed a significant anticancer activity against MCF-7 cell line⁶⁶. Here, the IC₅₀ value for both the breast cancer cell lines (6.44 ± 0.045 and 5.87 ± 0.031 µg/mL respectively) was much lower than as that found in case of EER, which indicates more efficacy of GNPs than EER. The overview of the IC₅₀ value is presented in the Table 1. In this study, it was found that similar to EER, GNPs also showed stronger toxicity to MDA-MB 231 (TNBC) cell lines (Figs. 7 and 8). However, as that of EER, the cell viability decreased with the increase of concentrations of GNPs (Fig. 8). The cytotoxic efficiency of GNPs might be more due to their surface properties and small size. Due to the charge differences between cell membrane (negatively charged) and the GNPs (positively charged) it can interact with the cell membrane of the cancerous cells and interferes the cell permeability. Thereby, it enters into the mitochondria and damage the electron transport system. It also produces a high-level of ROS and ultimately through DNA damage and apoptosis, the cells death occurs.

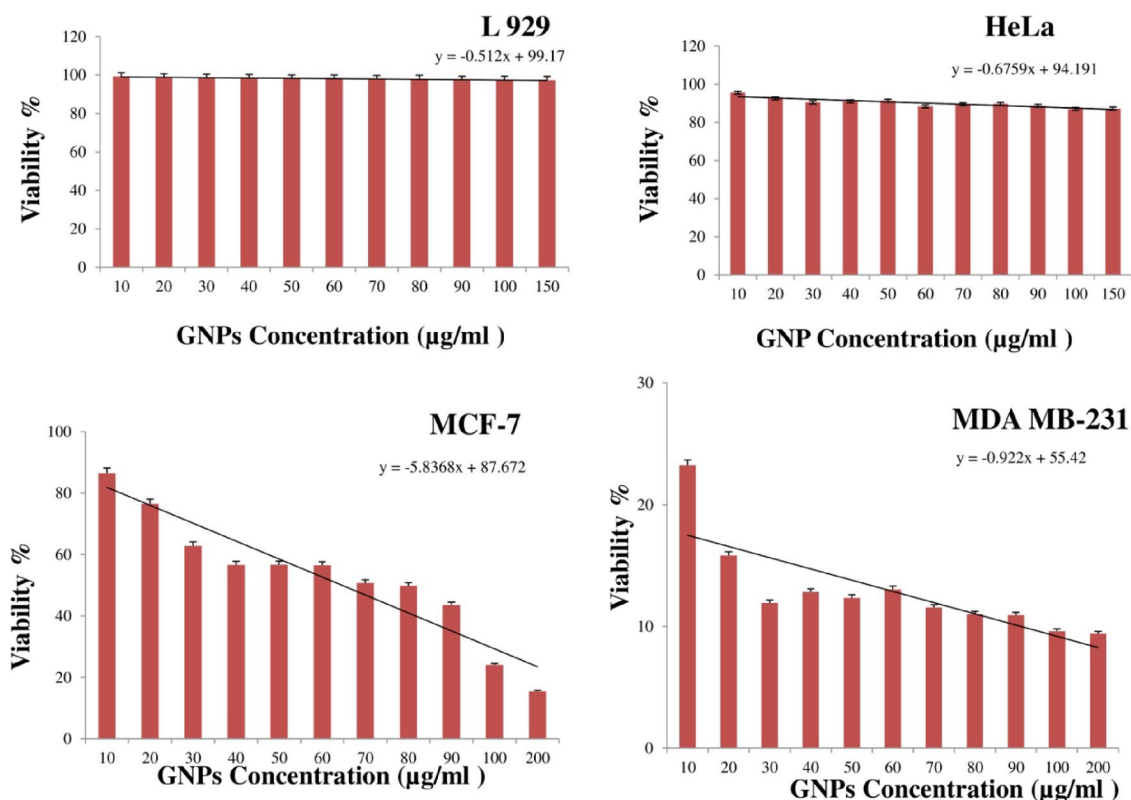


Figure 7. Cytotoxicity of GNPs on HeLa, L929, MDA MB-231 and MCF-7 cell lines.

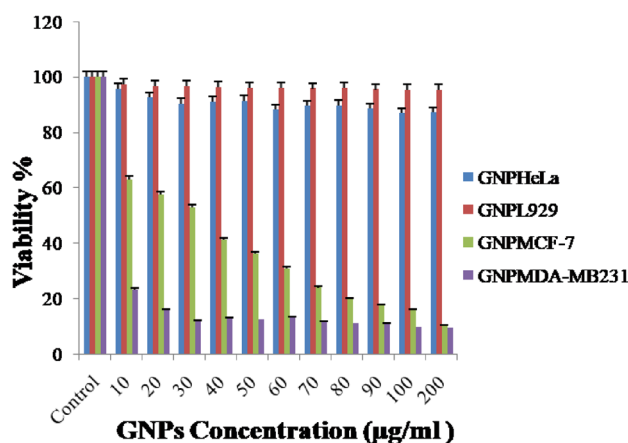


Figure 8. Effect of different concentrations of GNPs and negative control on HeLa, L929, MDA MB-231 and MCF-7 cell lines.

(52). In our investigation, as GNPs showed more potential towards TNBC cell lines, with further exploration of its effectiveness, specificity and underlying molecular mechanism might help in development of personalised medicine for treatment of this deleterious disease.

Conclusion

In the present investigation, we aimed to demonstrate the selective cytotoxicity of *Curcuma caesia* rhizome extract and its mediated gold nanoparticles towards breast cancer cell lines (MCF-7 and MDA MB-231), while assessing their general cytotoxic potential on other cancerous and non-cancerous cell lines (HeLa, L929). In our study, it was found that the extract and the synthesized GNPs showed no cytotoxic effect on both HeLa, L929 cell lines. The extract and the GNPs epitomized specific potentiality against breast cancer cell lines. However, compared to the extract, GNPs showed more cytotoxicity against MCF-7 and MDA MB-231 cell lines. Moreover, compared to MCF-7, both the extract and the GNPs were found to be more toxic for MDA-MB 231. In our study, it was

also observed that the synthesized GNPs showed more potentiality towards MDA-MB 231 toxicity compared to the extract. Therefore, the synthesized GNPs might be used for target specific cancer treatment. Combination of traditional medicine with such nanomaterial might provide a better opportunity for development of new anti-breast cancer agents. Nevertheless, based on this preliminary data, further investigation is needed to elucidate the molecular mechanism behind the breast cancer specificity (especially for TNBC) of the rhizome of this endangered species and GNPs synthesized by its extract.

Materials and methods

Materials

All chemicals required to carry out this experiment such as Ethanol, HAuCl_4 aqueous solution, Dulbecco's modified eagle medium, 3-(4,5-dimethylthiazol-2-yl)-2,5-diphenyltetrazolium bromide [MTT], Dimethylsulphoxide were obtained from Sigma (Bangalore, India) and Merk (Mumbai, India) and were of analytical grade and of high purity (more than 99%). Cell lines used in this study were procured from National Centre for Cell Sciences (Pune, India). The rhizome of *Curcuma caesia* Roxb. (Black turmeric) was collected from R&D division, NEDFi, Khetri (Assam, India) following the guidelines of National Biodiversity Authority, India. The rhizome was collected during the month of April and was authenticated by Dr. Sauravjyoti Borah, Curator, Department of Botany, Gauhati University, Assam, India. The voucher specimen had been submitted to the herbarium of Department of Botany, Gauhati University and the Accession No. of the specimen is GUBH20605.

Methods

Preparation of ethanolic extract of rhizome (EER)

The collected rhizome of *Curcuma caesia* Roxb. was thoroughly washed with double distilled water for several times to remove dust and sliced into small pieces. The sliced pieces were shade dried in a dust free condition for about two months at room temperature. Dried pieces were grinded using a mixer grinder (Model: Bajaj GX 11, Mumbai, India) and strained 3–4 times to get fine powder. For preparation of extract, the fine powders were dissolved in ethanol in the ratio of 1:3(w/v) and incubated in a shaking incubator (100 rpm, 25 °C and 72 h.). The ethanolic extract of the rhizome (EER) was obtained by filtering the mixture. The filtered extract was dried by using rotary evaporator (Rotera Equitron, Make: MedicalInstrument Mfg. Co., Mumbai, India) and lyophilizer. The lyophilized powder was stored at 4°C for further study.

Cytotoxicity of EER

Sample preparation

Stock solution of EER was prepared by mixing 160 mg of lyophilized powder in 1 mL of DMSO (Dimethylsulphoxide). The stock solution was filter sterilized and different concentrations of the extract (ranging from 0.5 to 500 µg/mL) were prepared from it. These concentrations were used for cytotoxic analysis.

In case of GNPs, stock solution was prepared for cytotoxic study by mixing the lyophilized powder of GNPs with plain DMEM (Dulbecco's modified eagle medium). Different concentrations of GNPs were prepared from the filter sterilized stock solution using plain DMEM and used for toxicity study.

Cell culture

Different cell lines such as HeLa (human cervical cancer), L 929 (normal rat fibroblast), MCF-7 (human breast cancer) and MDA MB-231 (triple negative breast cancer) were maintained in complete DMEM containing 0.1 mM non-essential amino acids, 1.5 g/L sodium bicarbonate, 2 mM L-glutamine and 1.0 mM sodium pyruvate supplemented with 10% fetal bovine serum (FBS; heat inactivated) and 1% antibiotic–antimycotic solution (1000 U/mL penicillin G, 10 mg/mL streptomycin sulphate, 5 mg/mL gentamycin and 25 µg/mL amphotericin B) in 25 and 75 cm² mammalian cell culture flasks. The cells were cultured by keeping the flasks in a CO₂ incubator (Heal Force, HF 160 W, Shanghai, China) at 37 °C, 90% relative humidity, 5% CO₂ and 95% air. When the cells approached 70–80% confluency, they were sub-cultured (passaged) with trypsin–EDTA and fresh medium into 25 cm² culture flasks.

Cytotoxicity assay

For cytotoxic assay of the EER, HeLa, L 929, MCF-7 and MDA MB-231 cells were seeded (100 µL each) in each well of four different 96-well flat bottom tissue culture plate (Cell Bind, Corning, Germany) and incubated in complete medium for 24 h in a CO₂ incubator under conventional culture condition (37 °C, 5% CO₂ and 90% relative humidity). After 24 h of incubation, the complete medium was replaced from each well with 100 µL of plain medium (serum free) that contained varied concentration of EER (except the control) such that DMSO content in each well was 1%. This was done to minimize the cytotoxic effects of DMSO. In case of control, 100 µL of plain medium without drug was added. For each concentration, four replications were maintained in every case. The plates were then incubated for another 24 h. After 24 h, the plain medium from each and every well was removed and the cells were washed with PBS (Phosphate buffer solution). Following this, 100 µL of MTT [3-(4,5-dimethylthiazol-2-yl)-2,5-diphenyltetrazolium bromide] prepared in plain medium (0.5 mg/mL) was added to each well and all the plates were incubated for 4 h. After incubation, the medium was removed without disturbing the formazan crystals (the living cells converted the soluble MTT salt into insoluble purple coloured formazan). After removal of the medium, 100 µL of DMSO was added to each well to dissolve the formazan crystals. The absorbance of formazan solution at 570 nm was determined by using a multiwell plate reader (Tecan microplate reader, model 680, California, USA). Cell viability was calculated by using the following formula.

$$\text{Cell viability (\%)} = (N_t/N_c) \times 100$$

where, N_t and N_c are the mean absorbance of treated and untreated cells respectively.

The IC_{50} (inhibition concentration) was determined from the graph of the number of viable cells against drug concentration.

Synthesis of GNPs

To synthesize GNPs, 0.8% (v/v) of EER was mixed with 0.875 mM $HAuCl_4$ (chlorauric acid) aqueous solution. The whole mixture was allowed to run for constant magnetic stirring (C-MAG-HS7, IKA®) at room temperature (25 °C) and observed for any colour change. The concentration of EER was optimized by mixing varying concentration of EER (0.2 to 1.2%, v/v) with 0.875 mM $HAuCl_4$ aqueous solution. The concentration of $HAuCl_4$ was optimized by reacting varying concentration of $HAuCl_4$ (0.250–1.125 mM) with 0.8% (v/v) of EER. Optimization of reaction time was done by stirring the reaction mixture of 0.8% (v/v) of EER and 0.875 mM $HAuCl_4$ aqueous solution for different time period (1–4 h.). The final reaction volume was made up to 2 mL with double distilled water in each case.

Characterization of GNPs

UV–VIS absorbance spectroscopy

The absorption spectra of the reaction mixture were scanned at the wavelength between 200 and 900 nm on a Tecan Infinite M200 UV–VIS spectrophotometer and thus synthesis of GNPs was confirmed.

Transmission electron microscopy (TEM)

TEM analysis was carried out on a JEOL 2100 UHRTEM microscope. For TEM analysis, samples were prepared by drying a carbon coated copper grid on which the GNPs solution coated by putting two or three drops over it. Morphology, crystalline nature and size distribution of GNPs were analysed by TEM.

X-ray diffraction (XRD) analysis

Crystalline nature of the synthesized GNPs was confirmed from X-ray diffractograms (XRD). XRD was studied on a Bruker D8 ADVANCE X-ray powder diffractometer (Bruker AXS Inc.) operating at 45 kV and 45 mA with Cu source at 1.54 Å wavelength.

Fourier transform infrared spectroscopy (FTIR)

Interactions of EER with GNPs were analysed in the range of 450–4000 cm^{-1} by using a FT-IR spectrophotometer (Shimadzu IR Affinity 1).

Thermo gravimetric analysis (TGA) analysis

Capping behaviour of the phytochemicals present in EER with GNPs were studied using Thermogravimetric analyzer (TGA) (Model: TGA-7, Perkin-Elmer).

Cytotoxicity of GNPs

Same procedure was followed for the cytotoxicity study of GNPs as that of EER. In this case also four different cell lines (HeLa, L 929, MCF-7 and MDA MB-231 respectively) were used. The drug used was different concentrations of GNPs.

Data availability

All data generated or analysed during this study are included in this manuscript [and its supplementary information files].

Received: 11 January 2024; Accepted: 27 June 2024

Published online: 26 July 2024

References

1. Ravindran, P. N., Nirmal, B. K. & Sivaraman, K. *Turmeric: The Genus Curcuma* 11 (CRC Press, 2007).
2. Sasikumar, B. Genetic resources of Curcuma: Diversity, characterization and utilization. *Plant Genet. Resour.* **3**(2), 230–251. <https://doi.org/10.1079/PGR200574> (2005).
3. Charles, S. V., Elias, U. M., Ramachandram, T. R. & Kamada, T. Secondary metabolites from rhizome of *Curcuma caesia* Roxb. (Zingiberaceae). *Biochem. Syst. Ecol.* **48**, 107–110. <https://doi.org/10.1016/j.bse.2012.11.008> (2013).
4. Mahato, D. & Sharma, H. P. Kali Haldi, an ethnomedicinal plant of Jharkhand state: A review. *Indian J. Tradit. Knowl.* **17**(2), 322–326. <https://doi.org/10.4103/1477-3163.133520> (2018).
5. Devi, H. P., Mazumder, P. B. & Devi, L. P. Antioxidant and antimutagenic activity of *Curcuma caesia* Roxb. rhizome extracts. *Toxicol. Rep.* **2**, 423–428. <https://doi.org/10.1016/j.toxrep.2014.12.018> (2015).
6. Baghel, S. S., Baghel, R. S., Sharma, K. & Sikarwar, I. Pharmacological activities of *Curcuma caesia*. *Int. J. Green Pharm.* **7**(1), 1–5. <https://doi.org/10.4103/0973-8258.111590> (2013).
7. Karmakar, I., Dolai, N., Bala, A. & Halder, P. K. Anxiolytic and CNS depressant activities of methanol extract of *Curcuma caesia* rhizome. *Pharmacology* **2**, 738–747. https://doi.org/10.1300/J157v06n03_06 (2011).
8. Arulmozhi, D. K., Sridhar, N., Veeranjanyulu, A. & Arora, S. K. Preliminary mechanistic studies on the smooth muscle relaxant effect of hydroalcoholic extract of *Curcuma caesia*. *J. Herb. Pharmacother.* **6**, 117–124. https://doi.org/10.1080/j157v06n03_06 (2006).
9. National Medicinal Plants Board. *Agro-Techniques of Selected Medicinal Plants* (The Energy and Resources Institute Press, 2008).

10. Chiu, T. L. & Su, C. C. Curcumin inhibits proliferation and migration by increasing the Bax to Bcl-2 ratio and decreasing NF-kappaBp65 expression in breast cancer MDA-MB-231 cells. *Int. J. Mol. Med.* **23**, 469–475. https://doi.org/10.3892/ijmm_00000153 (2009).
11. Liu, Q., Loo, W. T., Sze, S. C. & Tong, Y. Curcumin inhibits cell proliferation of MDA-MB-231 and BT-483 breast cancer cells mediated by down-regulation of NFkappaB, cyclinD and MMP-1 transcription. *Phytomedicine* **16**, 916–922. <https://doi.org/10.1016/j.phymed.2009.04.008> (2009).
12. Mohammad, A. A., Eltayeb, N. M., Khairuddean, M. & Salhimia, S. M. Bioactive chemical constituents from *Curcuma caesia* Roxb. rhizomes and inhibitory effect of curcuzederone on the migration of triple-negative breast cancer cell line MDA-MB-231. *Nat. Res. Prod.* **35**(18), 3166–3170. <https://doi.org/10.1080/14786419.2019.1690489> (2019).
13. Liu, H. T. & Ho, Y. S. Anticancer effect of curcumin on breast cancer and stem cells. *Food Sci. Hum. Wellness* **7**(2), 134–137. <https://doi.org/10.1016/j.fshw.2018.06.001> (2018).
14. Krmakar, L., Dolai, N., Suresh, K. R. B. & Halder, P. K. Antitumor activity and antioxidant property of *Curcuma caesia* against Ehrlich ascites carcinoma bearing mice. *Pharma Biol.* **51**(6), 753–759. <https://doi.org/10.3109/13880209.2013.764538> (2013).
15. Kumar, S., Dubey, K. K., Tripathi, S., Fujii, M. & Misra, K. Design and synthesis of curcumin-bioconjugates to improve systemic delivery. *Nucleic Acids Symp. Ser.* **44**, 75–76. <https://doi.org/10.1093/nass/44.1.75> (2000).
16. Hadem, K. L. H., Sharan, R. N. & Kma, L. Phytochemicals of *Aristolochiatagala* and *Curcuma caesia* exert anticancer effect by tumor necrosis factor- α -mediated decrease in nuclear factor kappa B binding activity. *J Basic Clin. Pharm.* **7**(1), 1–11. <https://doi.org/10.4103/0976-0105.170585> (2015).
17. Prasad, R.; Patnaik, S. Conservation Assessment and Management Planning. *Proceeding of the Conservation Assessment and Management Planning (CAMP) Workshop for Non timber forest products in Madhya Pradesh* 1–99 (Indian Institute of Forest Management, 1998).
18. Salem, S. S. A mini review on green nanotechnology and its development in biological effects. *Arch. Microbiol.* **205**, 128. <https://doi.org/10.1007/s00203-023-03467-2> (2023).
19. Ventola, C. L. The nanomedicine revolution: Part 1: Emerging concepts. *Pharm. Ther.* **37**(9), 512–525 (2012).
20. Afzal, O., Altamimi, A. S. A. & Nadeem, M. S. Nanoparticles in drug delivery: From history to therapeutic applications. *Nanomaterials (Basel)*. **12**(24), 4494. <https://doi.org/10.3390/nano12244494> (2022).
21. Vollath, D., Fischer, F. D. & Holec, D. Surface energy of nanoparticles: Influence of particle size and structure. *Beilstein J. Nanotechnol.* **9**, 2265–2276. <https://doi.org/10.3762/bjnano.9.211> (2018).
22. Sharma, K. P. et al. Nanotechnology and its application: A review nanotechnology. In *Cancer Management Precise Diagnostics Toward Personalized Health Care* 1–33 (Elsevier, 2021).
23. Das, A. K. et al. Papaya latex mediated synthesis of prism shaped proteolytic gold nanozymes. *Sci. Rep.* **13**, 5965. <https://doi.org/10.1038/s41598-023-32409-7> (2023).
24. Oberdörster, G., Oberdörster, E. & Oberdörster, J. Nanotoxicology: An emerging discipline evolving from studies of ultrafine particles. *Environ. Health Perspect.* **113**, 823–839. <https://doi.org/10.1289/ehp.7339> (2005).
25. Cui, D., Tian, F., Ozkan, C. S., Wang, M. & Gao, H. Effect of single wall carbon nanotubes on human HEK293 cells. *Toxicol. Lett.* **155**, 73–85. <https://doi.org/10.1016/j.toxlet.2004.08.015> (2005).
26. Gupta, D., Yadav, P., Garg, D. & Gupta, T. K. Pathways of nanotoxicity: Modes of detection, impact, and challenges. *Front. Mater. Sci.* **15**, 512–542 (2021).
27. Li, J. J., Hartono, D., Ong, C. N., Bay, B. H. & Yung, L. Y. Autophagy and oxidative stress associated with gold nanoparticles. *Biomaterials* **31**(23), 5996–6003. <https://doi.org/10.1016/j.biomaterials.2010.04.014> (2010).
28. Wei, P., Zhang, L., Lu, Y., Man, N. & Wen, L. C60(Nd) nanoparticles enhance chemotherapeutic susceptibility of cancer cells by modulation of autophagy. *Nanotechnology* **21**(49), 495101. <https://doi.org/10.1088/0957-4484/21/49/495101> (2010).
29. Yamawaki, H. & Iwai, N. Cytotoxicity of water-soluble fullerene in vascular endothelial cells. *Am. J. Physiol. Cell Physiol.* **290**, 1495. <https://doi.org/10.1152/ajpcell.00481.2005> (2006).
30. Zhang, Q. et al. Autophagy-mediated chemosensitization in cancer cells by fullerene C60 nanocrystal. *Autophagy* **5**(8), 1107–1117. <https://doi.org/10.4161/auto.5.8.9842> (2009).
31. Seleverstov, O. et al. Quantum dots for human mesenchymal stem cells labelling. A size-dependent autophagy activation. *Nano Lett.* **6**, 2826–2832. <https://doi.org/10.1021/nl0619711> (2006).
32. Stern, S. T. et al. McNeil induction of autophagy in porcine kidney cells by quantum dots: A common cellular response to nanomaterials?. *Toxicol. Sci.* **106**(1), 140–152. <https://doi.org/10.1093/toxsci/kfn137> (2008).
33. Ankamwar, B. et al. Biocompatibility of Fe₃O₄ nanoparticles evaluated by in vitro cytotoxicity assays using normal, glia and breast cancer cells. *Nanotechnology* **21**, 075102. <https://doi.org/10.1088/0957-4484/21/7/075102> (2010).
34. Hong, H. et al. Cancer-targeted optical imaging with fluorescent zinc oxide nanowires. *Nano Lett.* **11**(9), 3744–3750. <https://doi.org/10.1021/nl201782m> (2011).
35. Dreaden, E. C., Mackey, M. A., Huang, X., Kang, B. & El-Sayed, M. A. Beating cancer in multiple ways using nanogold. *Chem. Soc. Rev.* **40**, 3391–3404. <https://doi.org/10.1039/C0CS00180E> (2011).
36. El-Sayed, M. A. Some interesting properties of metals confined in time and nanometer space of different shapes. *AccChem Res.* **34**(4), 257–264. <https://doi.org/10.1021/ar960016n> (2001).
37. Pan, Y. et al. Gold nanoparticles of diameter 1.4 Nm trigger necrosis by oxidative stress and mitochondrial damage. *Small* **5**, 2067–2076. <https://doi.org/10.1002/sml.200900466> (2009).
38. Chen, Y. S., Hung, Y. C., Liao, I. & Huang, G. S. Assessment of the in vivo toxicity of gold nanoparticles. *Nanoscale Res. Lett.* **4**, 858. <https://doi.org/10.1007/s11671-009-9334-6> (2009).
39. Sani, A., Cao, C. & Cui, D. Toxicity of gold nanoparticles (AuNPs): A review. *Biochem. Biophys. Rep.* **26**, 10991. <https://doi.org/10.1016/j.bbrep.2021.100991> (2021).
40. Zhang, X. D. et al. In vivo renal clearance, biodistribution, toxicity of gold nanoclusters. *Biomaterials* **33**, 4628–4638. <https://doi.org/10.1016/j.biomaterials.2012.03.020> (2012).
41. Meng, J. et al. Using gold nanorods core/silver shell nanostructures as model material to probe biodistribution and toxic effects of silver nanoparticles in mice. *Nanotoxicology*. **8**, 686–696. <https://doi.org/10.3109/17435390.2013.822593> (2014).
42. Chan, H. & Král, P. Nanoparticles self-assembly within lipid bilayers. *ACS Omega* **3**, 10631–10637. <https://doi.org/10.1021/acsomega.8b01445> (2018).
43. Joshi, P. et al. The anticancer activity of chloroquine-gold nanoparticles against MCF-7 breast cancer cells. *Colloids Surf. B* **95**, 195–200. <https://doi.org/10.1016/j.colsurfb.2012.02.039> (2012).
44. Das, R. K., Sharma, P., Nahar, P. & Bora, U. Synthesis of gold nanoparticles using aqueous extract of *Calotropisprocera* latex. *Mater. Lett.* **65**, 610–613. <https://doi.org/10.1016/j.matlet.2010.11.040> (2011).
45. Bar, H. et al. synthesis of silver nanoparticles using latex of *Jatropha curcas*. *Colloids Surf. A* **339**, 134–139. <https://doi.org/10.1016/j.colsurfa.2009.02.008> (2009).
46. Khan, F. et al. Green nanotechnology: Plant-mediated nanoparticle synthesis and application. *Nanomaterials* **12**, 673. <https://doi.org/10.3390/nano12040673> (2022).
47. Swilam, N. & Khaled, A. N. Polyphenols profile of pomegranate leaves and their role in green synthesis of silver nanoparticles. *Sci. Rep.* **10**, 14851. <https://doi.org/10.1038/s41598-020-71847-5> (2020).
48. Glusker, J., Katz, A., Bock, C. & Rigaku, J. Metal ions in biological systems. *Chem. Biol.* **16**(2), 8–16 (1999).

49. Si, S. & Mandal, T. K. Tryptophan-based peptides to synthesize gold and silver nanoparticles: A mechanistic and kinetic study. *Chemistry* **13**(11), 3160–3168. <https://doi.org/10.1002/chem.200601492> (2007).
50. Akinfenwa, A. O. & Hussein, A. A. Phyto-metallic nanoparticles: Biosynthesis, mechanism, therapeutics, and cytotoxicity. In *Toxicity of Nanoparticles: Recent Advances and New Perspectives* (IntechOpen, 2023).
51. Kavaz, D., Huzaifa, U. & Zimuto, T. Biosynthesis of Gold nanoparticles using *Scytosiphon lomentaria* (Brown algae) and *Spyridia filamentosa* (Red algae) from Kyrenia Region and evaluation of their antimicrobial and antioxidant activity. *Haceteppe J. Biol. Chem.* **47**(4), 367–382 (2019).
52. Bharadwaj, K. K. *et al.* Green synthesis of gold nanoparticles using plant extracts as beneficial prospect for cancer theranostics. *Molecules* **26**, 6389. <https://doi.org/10.3390/molecules26216389> (2021).
53. Rahimi, H. R., Nedaeinia, R., Shamloo, A. S., Nikdoust, S. & Oskuee, R. K. Novel delivery system for natural products: Nano-curcumin formulations. *Avicenna J. Phytomed.* **6**(4), 383–398. <https://doi.org/10.22038/AJP.2016.6187> (2016).
54. Lesner, S. & Cotran, R. Breast cancer. In *Robbins Pathologic Basis of Diseases* (eds Cotran, R. *et al.*) 1093–1120 (. Sounders, 1999).
55. World Cancer Report. International Agency for Research on Cancer (2008).
56. Ferlay, J. *et al.* Estimates of the cancer incidence and mortality in Europe in 2006. *Ann. Oncol.* **18**(3), 581–592. <https://doi.org/10.1093/annonc/mdl498> (2007).
57. Abdelhamed, S. *et al.* Identification of plant extracts sensitizing breast cancer cells to TRAIL. *Oncol. Rep.* **29**(5), 1991–1998. <https://doi.org/10.3892/or.2013.2293> (2013).
58. Umar, H. *et al.* Prediction of cell migration potential on human breast cancer cells treated with Albizia lebbeck ethanolic extract using extreme machine learning. *Sci. Rep.* **13**(1), 22242. <https://doi.org/10.1038/s41598-023-49363-z> (2023).
59. Hadisaputri, Y. E. *et al.* Antiproliferation activity and apoptotic mechanism of soursop (*Annona muricata* L.) leaves extract and fractions on MCF7 breast cancer cells. *Breast Cancer* **16**(13), 447–457. <https://doi.org/10.2147/BCTT.S317682> (2021).
60. Pal, A., Sanyal, S., Das, S. & Sengupta, T. K. Effect of Lantana camara ethanolic leaf extract on survival and migration of MDA-MB-231 triple-negative breast cancer cell line. *J. Herb. Med.* **43**, 100837. <https://doi.org/10.1016/j.hermed.2023.100837> (2024).
61. Omrani, V. F. *et al.* Effects of sambucus ebulus extract on cell proliferation and viability of triple-negative breast cancer: An in vitro and in vivo study. *Anticancer Agents Med. Chem.* **22**(7), 1386–1396. <https://doi.org/10.2174/1871520621666210412113944> (2022).
62. Suffness, M. & Pezzuto, J. M. Assays related to cancer drug discovery. In *Assays for Bioactivity (Methods in Plant Biochemistry Vol. 6* (ed. Hostettmann, K.) 71–133 (Academic Press, 1990).
63. Abdel-Hameed, E. S., Salih, A., Bazaid, S. A. & El-Sayed, M. M. Phytochemical studies and evaluation of antioxidant, anticancer and antimicrobial properties of *Conocarpus erectus* L. growing in Taif, Saudi Arabia. *Eur. J. Med. Plants* **2**, 93–112. <https://doi.org/10.9734/EJMP/2012/1040> (2012).
64. Abdelhamed, S. *et al.* Identification of plant extracts sensitizing breast cancer cells to TRAIL. *Oncol. Rep.* **29**(5), 2293. <https://doi.org/10.3892/or.2013.2293> (2013).
65. Umar, H. & Aliyu, M. R. *Moringa oleifera*-mediated iron oxide nanoparticles, characterization and their anti-proliferative potential on MDA-MB 231 human breast cancer cells. *Pak. J. Pharm. Sci.* **36**(6), 1875–1883 (2023).
66. Abed, S. A., Mohammed, M. A. & Khalaf, H. Y. Novel photothermal therapy using platinum nanoparticles in synergy with near-infrared radiation (NIR) against human breast cancer MCF-7 cell line. *Results Chem.* **4**(1–2), 100591. <https://doi.org/10.1016/j.rechem.2022.100591> (2022).

Acknowledgements

We thank and acknowledge Department of Biotechnology, Ministry of Science and Technology, Govt. of India for providing funding support for this work. AKD would like to thank Biotech Hub, Centre for Environment, Indian Institute of Technology, Guwahati for providing necessary facilities for carrying out the experiments.

Author contributions

Conceived and designed the experiments: Ajoy K Das, Utpal Bora. Performed the experiments: Ajoy K Das. Analyzed the data: Ajoy K Das, Maina Borah, Jon Jyoti Kalita and Utpal Bora. Contributed to the writing of the manuscript: Utpal Bora, Ajoy K Das, Maina Borah and Jon Jyoti Kalita.

Competing interests

The authors declare no competing interests.

Additional information

Supplementary Information The online version contains supplementary material available at <https://doi.org/10.1038/s41598-024-66175-x>.

Correspondence and requests for materials should be addressed to A.K.D. or U.B.

Reprints and permissions information is available at www.nature.com/reprints.

Publisher's note Springer Nature remains neutral with regard to jurisdictional claims in published maps and institutional affiliations.



Open Access This article is licensed under a Creative Commons Attribution-NonCommercial-NoDerivatives 4.0 International License, which permits any non-commercial use, sharing, distribution and reproduction in any medium or format, as long as you give appropriate credit to the original author(s) and the source, provide a link to the Creative Commons licence, and indicate if you modified the licensed material. You do not have permission under this licence to share adapted material derived from this article or parts of it. The images or other third party material in this article are included in the article's Creative Commons licence, unless indicated otherwise in a credit line to the material. If material is not included in the article's Creative Commons licence and your intended use is not permitted by statutory regulation or exceeds the permitted use, you will need to obtain permission directly from the copyright holder. To view a copy of this licence, visit <http://creativecommons.org/licenses/by-nc-nd/4.0/>.

© The Author(s) 2024